Nonlocal Landau free-energy functional: Application to the magnetic phase transition in $CsNiF_3$

M. L. Plumer and A. Caillé
Centre de Recherche en Physique du Solide et Département de Physique, Université de Sherbrooke, Sherbrooke, Québec, Canada J1K 2R1
(Received 24 June 1987; revised manuscript received 24 September 1987)

A general nonlocal Landau-type, free-energy functional which includes magnetoelastic coupling is described and used to study thermodynamic properties associated with the magnetic phase transition in $CsNiF_3$. One of the possible magnetically ordered phases obtained by an analysis of the phenomenological free energy is the experimentally observed three-domain antiferromagnetic structure. Explicit expressions are also derived for the magnetic phase diagram, field dependence of the magnetization, anomalies in thermal expansion and the elastic constants, and stress dependence of the Néel temperature and magnetostriction. Magnetic-field-induced domain reorientation effects on these quantities are emphasized. Predictions of the theory which can be compared with available experimental data show good agreement.

I. INTRODUCTION

Phenomenological Landau-type free energies form the basis of many mean-field descriptions of properties associated with phase transitions in a wide variety of materials.[1] This approach has been used to a great extent to provide a theory of magnetic and structural phase transitions in solids and is able to describe the many different kinds of ordering which can occur,[1,2] e.g., homogeneous and inhomogeneous, commensurate and incommensurate modulations, single and multicomponent order parameters, etc. Fundamental expressions of the Landau free energy, obtained on the basis of symmetry considerations, must be flexible enough to account for all of these different types of phase transitions.

Most applications of Landau theory begin with a free energy specific to the material and type of ordering under investigation and rely on physical arguments (often unstated) to have reduced the problem to its simplest expression. This procedure is not always obvious and leaves some doubt regarding the completeness of the description. A more formal procedure for writing the free energy is usually desirable. In this work, the formulation based on symmetry arguments is generalized for writing the Landau free energy in a *nonlocal* form[3] appropriate for the study of materials (with a center of inversion symmetry) exhibiting a magnetic phase transition. Coupling of the order parameter to the elastic strain tensor is included and comments are made regarding the extension of this approach to other systems. The remainder (and bulk) of this work is devoted to an application of this Landau theory to study a variety of magnetic and elastic properties associated with the magnetic phase transition in $CsNiF_3$. The formalism presented here also serves as a foundation for the investigation of properties associated with phase transitions in related materials (see below). We have recently used it to study the magnetic phase diagram of $CsNiCl_3$ and further applications are in progress. For this purpose, a detailed (and somewhat lengthy) presentation of the theory will be given here.

$CsNiF_3$ is a member of a large class of materials with the generic chemical formula ABX_3, whose hexagonal structures at high temperature are closely related to each other and show a great diversity of structural and magnetic propreties at low temperatures.[4–8] The quasi-one-dimensional nature of the low-temperature magnetic interactions in $CsNiF_3$ (and some related magnetic compounds) has been of interest in the recent past.[9] Ferromagnetic short-range order of magnetic-ion moments in chains parallel to the c axis[10] is observed at temperatures $T \lesssim 80$ K. A large single-ion magnetic anisotropy[11] between directions parallel and perpendicular to the c axis confines the moments to lie in the hexagonal basal plane. At a temperature $T \simeq 2.65$ K, there is a phase transition characterized by a three-dimensional ordering of the Ni^{2+} magnetic moments.[12,13] The ferromagnetic character of the spins along the c axis remains, and there is an onset of antiferromagnetic ordering in the basal plane. In the absence of an applied magnetic field, the basal-plane ordering consists of a three-domain structure, where the spins are directed along one of the three basal-plane crystallographic axes, as shown in Fig. 1. The effect of applying a magnetic field perpendicular to one of the spin directions is to increase the size of this domain relative to the other two.[13] A nearly single magnetic-domain crystal is achieved at a relatively small field of ~ 500 Oe. A further increase in field strength reduces the amplitude of the long-range order. The critical field H_c above which order is destroyed has been measured as a function of temperature.

The importance of relatively strong magnetic dipole interactions (comparable with exchange coupling) in the basal plane for stabilizing the observed magnetic structure was first demonstrated by Scherer and Barjhoux.[14] These authors used a model Heisenberg-type Hamiltonian which included nearest-neighbor exchange and dipole couplings as the basis for a mean-field calculation of the wave-vector dependent susceptibility. A similar approach was used by Suzuki,[15] where basal-plane dipole

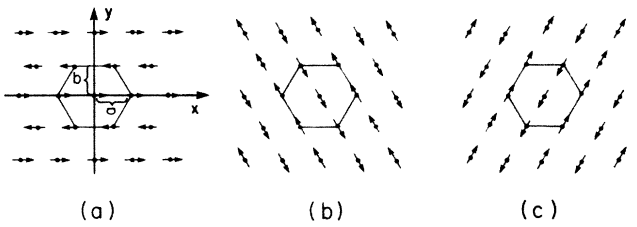

FIG. 1. Three-domain antiferromgnetic ordering of $CsNiF_3$ after Refs. 14 and 15 [where the moment directions corresponds to $\hat{\mathbf{S}}_1$ in Eq. (3.12)] and the wave vectors are given by (3.18).

interactions beyond nearest neighbor were included in a more extensive numerical analysis of the possible ordered states with similar results. Mean-field descriptions of this phase transition can be expected to be adequate outside a narrow critical region since strong, long-range, dipole interactions tend to suppress critical fluctuations.[16] This is evident in the results of critical neutron scattering, where a mean-field exponent $\beta=0.5$ is observed[12] at temperatures close to T_N: $2.45\ \mathrm{K} \lesssim T \lesssim 2.64\ \mathrm{K}$. The specific-heat data[17] at zero field is also compatible with a mean-field discontinuity, when allowance is made for the short-range contribution to the energy, except for an interval of 10^{-2} K near T_N, where the effects of critical fluctuations are evident.

The phenomenological free energy formulated in this work also describes the observed magnetic structure in $CsNiF_3$. Terms which have the form of a dipole interaction are shown to be responsible for the antiferromagnetic ordering, which serves to corroborate the conclusions of the above-mentioned theoretical studies. The field-induced magnetization and critical field $H_c(T)$ are also calculated within the framework of this theory and compared with available experimental data showing good agreement. A major focus of this work is the calculation of anomalous elastic behavior induced by the magnetic phase transition and magnetic-domain effects on these quantities. Expressions are presented for thermal expansion behavior, the elastic constants, field-induced magnetostriction and changes in the Néel temperature with applied stress. A variety of specific predictions which can be checked experimentally are made. In addition, the possibility of magnetization-induced inhomogeneous strain (lattice-displacement wave) is investigated.

The remainder of this paper is organized as follows. A formulation of the nonlocal free energy is given in Sec. II and is used in Sec. III to describe the magnetic phase transition in $CsNiF_3$. In Sec. IV magnetic-field effects are studied using the model free energy. Magnetoelastic-coupling-induced anomalous-strain effects are investigated in Sec. V and our conclusions are presented in Sec. VI.

II. NONLOCAL FREE ENERGY

In this section, a nonlocal Landau free-energy functional is introduced for the study of magnetic phase transitions in systems which have a center of inversion symmetry. Comments concerning the extension of this formalism for other types of phase transitions are also made.

It is assumed here that the physical properties of interest can be described by the state of the long-range magnetic ordering $\mathbf{s}(\mathbf{r})$, as well as the state of local strain $\tilde{e}_{\alpha\beta}(\mathbf{r})$ induced by the magnetic ordering. In its usual form, the free energy is written as an integral over a local energy density, which is expanded in powers of $\mathbf{s}(\mathbf{r})$ and its gradients. A gradient expansion is applicable only if $\mathbf{s}(\mathbf{r})$ can be chosen as uniform or as a slowly varying function in space (as is the case with many systems, e.g., incommensurate ordering). The following nonlocal free-energy functional is appropriate for the study of more general types of ordering (also see Ref. 18).

The amplitude of the long-range order is assumed to be small close to the phase transition, so that the free-energy functional may be expanded to low order of $\mathbf{s}(\mathbf{r})$. The requirement of invariance with respect to time-reversal symmetry ($\mathbf{s}\rightarrow-\mathbf{s}$) implies that only even powers of $\mathbf{s}(\mathbf{r})$ can appear. The coefficients of each term in this expansion are also assumed to depend only on differences between the space coordinates of the spins. Explicit coupling between $\mathbf{s}(\mathbf{r})$ and space coordinates must also be included in a general formulation of the free energy.

With these considerations, the free energy can be expressed by

$$F = F_s + F_{s\tilde{e}} + F_{\tilde{e}} , \tag{2.1}$$

where F_s is a functional of $\mathbf{s}(\mathbf{r})$ only, $F_{s\tilde{e}}$ is the contribution from magnetoelastic coupling and $F_{\tilde{e}}$ is the elastic energy. The important contributions to these terms for the purposes of this work are

$$F_s = \frac{1}{2V}\int d\mathbf{r}\int d\mathbf{r}'\, J_{\alpha\beta}(\tau)s_\alpha(\mathbf{r})s_\beta(\mathbf{r}') + \frac{1}{2V}\int d\mathbf{r}\int d\mathbf{r}'\, D_{\alpha\beta\gamma\delta}(\tau)\tau_\alpha\tau_\beta s_\gamma(\mathbf{r})s_\delta(\mathbf{r}')$$
$$+ \frac{1}{4V}\int d\mathbf{r}_1\int d\mathbf{r}_2\int d\mathbf{r}_3\int d\mathbf{r}_4\, B_{\alpha\beta\gamma\delta}(\mathbf{r}_1,\mathbf{r}_2,\mathbf{r}_3,\mathbf{r}_4)s_\alpha(\mathbf{r}_1)s_\beta(\mathbf{r}_2)s_\gamma(\mathbf{r}_3)s_\delta(\mathbf{r}_4) , \tag{2.2}$$

$$F_{s\tilde{e}} = \frac{1}{2V}\int d\mathbf{r}_1\int d\mathbf{r}_2\int d\mathbf{r}_3\, K_{\alpha\beta\gamma\delta}(\mathbf{r}_1,\mathbf{r}_2,\mathbf{r}_3)\tilde{e}_{\alpha\beta}(\mathbf{r}_1)s_\gamma(\mathbf{r}_2)s_\delta(\mathbf{r}_3) , \tag{2.3}$$

$$F_{\tilde{e}} = \frac{1}{2V}\int d\mathbf{r}\int d\mathbf{r}'\, \tilde{C}_{ij}(\tau)\tilde{e}_i(\mathbf{r})\tilde{e}_j(\mathbf{r}') , \tag{2.4}$$

where V is the volume of the crystal; the summation convention has been used with $\alpha,\beta,\gamma,\delta=x,y,z$ and in the Voigt notation $i,j=1-6$; $\tau=\mathbf{r}-\mathbf{r}'$; the coefficients B and K depend only on differences between pairs of coordinates. Inversion symmetry requires that $J(\tau)=J(-\tau)$ with corresponding relationships for the other coefficients. This symmetry also requires that only even powers of τ can appear. The structure of this phenomenological free-energy functional is analogous to some familiar microscopic Hamiltonians. The first term in (2.2) is a generalization of the anisotropic Heisenberg exchange model, and the second term has the form of the magnetic dipole-dipole interaction. Note also that the elastic energy is expressed as a functional of the local strain tensor which can be written as the sum of the usual uniform component plus an inhomogeneous part:

$$\tilde{e}_{\alpha\beta}(\mathbf{r})=e_{\alpha\beta}+\delta e_{\alpha\beta}(\mathbf{r}) \ . \tag{2.5}$$

The usual elastic constants are given by

$$C_{ij}=\int d\mathbf{r}\,\tilde{C}_{ij}(\mathbf{r}) \ . \tag{2.6}$$

Note that the explicit $\mathbf{r}$ dependence of the elastic coefficient $\tilde{C}_{ij}(\mathbf{r})$ is required for a complete description of inhomogeneous strain.

The symmetry arguments used to formulate the free energy (2.1)–(2.4) can be extended to account for other types of phase transitions. In crystals that do not possess a center of inversion symmetry, terms which are linear or cubic in τ are allowed. For many nonmagnetic phase transitions, terms which are cubic in the long-range order parameter must be included. Apart from these symmetry considerations, there are many higher-order terms, which could be important for some systems such as terms sixth order in $\mathbf{s}$ or terms which couple τ and the strain tensor.

The free energy F_s given by (2.2) can easily be reduced to a more familiar form for cases where $\mathbf{s}(\mathbf{r})$ is a slowly varying function. For simplicity, only terms isotropic in $\mathbf{s}$ and τ are retained, so that $J_{\alpha\beta}(\tau)=J(\tau)\delta_{\alpha\beta}$, with similar relations for D and B. These coefficients can then be expressed as a low-order gradient expansion, e.g.,

$$J(\tau)\simeq(J_0+J_2\nabla^2)\delta(\tau) \ , \tag{2.7}$$

where

$$J_0=\int d\tau J(\tau), \quad J_2=\tfrac{1}{2}\int d\tau\,\tau^2 J(\tau) \tag{2.8}$$

with similar expansions for Dr^2 and B. This leads to the usual local form

$$F=\frac{1}{2V}\int d\mathbf{r}(A_0+A_2\nabla^2)\mathbf{s}(\mathbf{r})\cdot\mathbf{s}(\mathbf{r}) + \frac{1}{4V}\int d\mathbf{r}\,B_0[\mathbf{s}(\mathbf{r})\cdot\mathbf{s}(\mathbf{r})]^2 \ , \tag{2.9}$$

where A_0 and A_2 contain contributions from both J and D terms. The assumption that $\mathbf{s}(\mathbf{r})$ is a slowly varying function is inappropriate for many systems (such as $CsNiF_3$) and the full nonlocal character of the free energy must be retained, as demonstrated below.

III. MAGNETIC PHASE TRANSITION IN $CsNiF_3$

A. Hexagonal symmetry

The free energy developed in Sec. II is shown in the following to account for the observed magnetic ordering of $CsNiF_3$ displayed in Fig. 1. Magnetoelastic couplings in this material are relatively weak (see Sec. V) and will not affect the analysis of the equilibrium magnetic properties described here and in Sec. IV, so that only the contribution to the free energy F_s given by (2.2) will be considered.

The space group of $CsNiF_3$ is $P6_3/mmc$ and the magnetic ions Ni^{2+} form a simple hexagonal lattice[19] with $a=6.23$ Å and $c=2.62$ Å (which is one-half the size of the chemical unit cell in the c direction), and the magnetic free energy must be invariant with respect to this symmetry. A result of this requirement is a contribution to F_s of the form $J_z s_z^2$ (also see Sec. IV B). Corresponding terms of this type in the magnetic Hamiltonian have been investigated[11] with the result that J_z is known to be large and positive, so that the free energy is minimized (for T close to T_N) with $s_z=0$. It will be assumed for the remainder of this work that the long-range ordered moments lie in the basal plane.

Terms in the free energy (2.2) invariant with respect to hexagonal symmetry can be chosen to have the following form (with $s_z=0$):

$$F_s=\frac{1}{2V}\int d\mathbf{r}\int d\mathbf{r}'\,J(\tau)\mathbf{s}(\mathbf{r})\cdot\mathbf{s}(\mathbf{r}')+\frac{1}{2V}\int d\mathbf{r}\int d\mathbf{r}'[D(\tau)\tau^2\mathbf{s}(\mathbf{r})\cdot\mathbf{s}(\mathbf{r}')+D_z(\tau)\tau_z^2\mathbf{s}(\mathbf{r})\cdot\mathbf{s}(\mathbf{r}')+d(\tau)\tau_\alpha\tau_\beta s_\alpha(\mathbf{r})s_\beta(\mathbf{r}')] + \frac{1}{4V}\int d\mathbf{r}_1\int d\mathbf{r}_2\int d\mathbf{r}_3\int d\mathbf{r}_4\,B(\mathbf{r}_1,\mathbf{r}_2,\mathbf{r}_3,\mathbf{r}_4)\mathbf{s}(\mathbf{r}_1)\cdot\mathbf{s}(\mathbf{r}_2)\mathbf{s}(\mathbf{r}_3)\cdot\mathbf{s}(\mathbf{r}_4) \ , \tag{3.1}$$

where each coefficient J, D, D_z, d, and B is independent. Note that this phenomenological free energy is more general than one which could be derived from a microscopic Hamiltonian which included only exchange and dipole interactions[15] since this would lead to $d(\tau)=-3D(\tau)$ and $D_z(\tau)=0$. The long-range ordering of the magnetic ions is described here by a quantity $\rho(\mathbf{r})$ which, for a local-moment model, is related to the spin density $\mathbf{s}(\mathbf{r})$ by the relation

$$\mathbf{s}(\mathbf{r})=\frac{V}{N}\sum_{\mathbf{R}}\rho(\mathbf{r})\delta(\mathbf{r}-\mathbf{R}) \ , \tag{3.2}$$

where $\mathbf{R}$ is a lattice vector and N is the number of N_i^{2+} ions. It is further assumed that $\rho(\mathbf{r})$ can be adequately represented by a single component of its Fourier expansion

$$\rho(\mathbf{r})=\mathbf{S}e^{i\mathbf{Q}\cdot\mathbf{r}}+\mathbf{S}^*e^{-i\mathbf{Q}\cdot\mathbf{r}} \ , \tag{3.3}$$

where S is the polarization vector and Q is the wave vector of the modulation, which is restricted to lie within the first Brillouin zone. Contributions to the free energy which are second and fourth order in S will be considered separately in Secs. III B and III C, respectively.

B. Second-order terms

Using (3.2) and (3.3) in (3.1) results in the following second-order contributions to the free energy:

$$F_s^{(2)}=(J_{\mathbf{Q}}+D_{\mathbf{Q}}+D_{z\mathbf{Q}})\mathbf{S}\cdot\mathbf{S}^*+\tfrac{1}{2}d_{\mathbf{Q}}^{\alpha\beta}(S_\alpha S_\beta^*+S_\alpha^* S_\beta)$$
$$+\tfrac{1}{2}[(J_{\mathbf{Q}}+D_{\mathbf{Q}}+D_{z\mathbf{Q}})(\mathbf{S}\cdot\mathbf{S}+\mathbf{S}^*\cdot\mathbf{S}^*)$$
$$+d_{\mathbf{Q}}^{\alpha\beta}(S_\alpha S_\beta+S_\alpha^* S_\beta^*)]\Delta_{2\mathbf{Q},\mathbf{G}_1}\,, \tag{3.4}$$

where $\alpha,\beta=x,y$,

$$J_{\mathbf{Q}}=\frac{V}{N}\sum_{\mathbf{R}}J(\mathbf{R})e^{i\mathbf{Q}\cdot\mathbf{R}}\,,$$
$$D_{\mathbf{Q}}=\frac{V}{N}\sum_{\mathbf{R}}D(\mathbf{R})R^2e^{i\mathbf{Q}\cdot\mathbf{R}}\,,$$
$$D_{z\mathbf{Q}}=\frac{V}{N}\sum_{\mathbf{R}}D_z(\mathbf{R})R_z^2e^{i\mathbf{Q}\cdot\mathbf{R}}\,, \tag{3.5}$$
$$d_{\mathbf{Q}}^{\alpha,\beta}=\frac{V}{N}\sum_{\mathbf{R}}d(\mathbf{R})R_\alpha R_\beta e^{i\mathbf{Q}\cdot\mathbf{R}}\,,$$

and

$$\frac{1}{N}\sum_{\mathbf{R}}e^{i2\mathbf{Q}\cdot\mathbf{R}}=\Delta_{2\mathbf{Q},\mathbf{G}_1} \tag{3.6}$$

has been used. Note that since Q must lie within the first Brillouin zone, $\mathbf{G}_1$ defined by (3.6) must be one of the shortest reciprocal lattice vectors in the hexagonal basal plane (if $\mathbf{Q}_z=0$):

$$\mathbf{G}_1=\pm\frac{2\pi}{b}\hat{\mathbf{y}},\pm\left[\frac{2\pi}{a}\hat{\mathbf{x}}\pm\frac{\pi}{b}\hat{\mathbf{y}}\right], \tag{3.7}$$

where $b=(3\frac{1}{2}/2)a$ and $\hat{\mathbf{x}},\hat{\mathbf{y}}$ are defined in Fig. 1.

Terms involving J can be expected to arise mainly from short-range exchange-type interactions so that nearest-neighbor couplings will dominate. From (3.5), these interactions give contributions to $J_{\mathbf{Q}}$ as follows:

$$J_{\mathbf{Q}}\simeq 2J_c\cos(cQ_z)+2J_a f(x,y) \tag{3.8}$$

with $J_c\equiv\tilde{J}(\mathbf{c})$, $J_a\equiv\tilde{J}(\mathbf{a})$, where $\tilde{J}(\mathbf{R})=(V/N)J(\mathbf{R})$ and

$$f(x,y)=\cos(x)+2\cos(\tfrac{1}{2}x)\cos(y) \tag{3.9}$$

with $x=aQ_x$, $y=bQ_y$. The observed ferromagnetic ordering along the c axis $Q_z=0$ is thus seen to minimize this term if J_c is negative. From an analysis of the corresponding term in a Heisenberg-type Hamiltonian, it has been concluded[11,14,15] that this coefficient is indeed negative, as well as large in magnitude. Note that antiferromagnetic ordering along the c axis ($Q_z=\pi/c$) results if $J_c>0$, as observed in, e.g., $CsNiCl_3$ (see Ref. 7).

The exchange interaction between the ferromagnetically coupled c-axis chains is very weak (Refs. 14 and 17) $J_a/J_c\sim 10^{-2}$, so that contributions to the free energy from the terms D, D_z, and d can be important for determining the basal-plane magnetic ordering. There is evidence from previous theoretical studies[14,15] that an important microscopic origin of these terms is magnetic dipole coupling, so that the possibility these interactions are long range cannot be ignored. With the reasonable assumption that these interaction are isotropic in the basal plane, we write $D(\mathbf{R})=D(R_\parallel,R_\perp)$, where $\mathbf{R}_\parallel$ and $\mathbf{R}_\perp$ are the components of R parallel and perpendicular to the c axis, with similar relations for D_z and d. Using $\mathbf{R}=\mathbf{R}_\perp+mc$ along with the definitions (3.5), we can write

$$D_{\mathbf{Q}}=D_c+\sum_{\mathbf{R}_\perp}\tilde{D}(R_\perp)e^{i\mathbf{Q}\cdot\mathbf{R}_\perp}\,,$$
$$D_{z\mathbf{Q}}=\sum_{\mathbf{R}_\perp}\tilde{D}_z(R_\perp)e^{i\mathbf{Q}\cdot\mathbf{R}_\perp}\,, \tag{3.10}$$
$$d_{\mathbf{Q}}^{\alpha,\beta}=a^{-2}\sum_{\mathbf{R}_\perp}\tilde{d}(R_\perp)R_\alpha R_\beta e^{i\mathbf{Q}\cdot\mathbf{R}_\perp}\,,$$

where (also see Ref. 14)

$$D_c=2\frac{V}{N}\sum_{m=1}D(0,mc)m^2c^2\cos(mcQ_z)\,,$$
$$\tilde{D}(R_\perp)=2\frac{V}{N}\sum_m D(R_\perp,mc)(R_\perp^2+m^2c^2)\cos(mcQ_z)$$
$$+\frac{V}{N}D(R_\perp,0)R_\perp^2\,,$$
$$\tilde{D}_z(\mathbf{R}_\perp)=2\frac{V}{N}\sum_m D_z(R_\perp,mc)m^2c^2\cos(mcQ_z)\,, \tag{3.11}$$
$$\tilde{d}(\mathbf{R}_\perp)=2a^2\frac{V}{N}\sum_m d(R_\perp,mc)\cos(mcQ_z)$$
$$+a^2\frac{V}{N}d(R_\perp,0)$$

with $Q_z=0$ for $CsNiF_3$.

Suzuki[15] determined the possible magnetic orderings for $CsNiF_3$-type systems as a function of the relative strengths of the nearest-neighbor interchain exchange coupling [corresponding to $2\tilde{J}(\mathbf{a})$] and the magnetic dipole strength in a model based on a Heisenberg-type Hamiltonian. One can infer from his paper that a large number of neighbor interactions were included in the numerical calculation. The phenomenological free energy $F_s^{(2)}$ is a generalization of his model, but contains the same symmetry properties, so that similar results must be obtained from its minimization. Instead of essentially repeating his calculation, we choose to demonstrate here some of the properties of the free energy with only nearest-neighbor couplings in the basal plane included. Corresponding results using up to third-neighbor interactions are presented in the Appendix. This calculation also serves to generalize the results of the nearest-neighbor dipole-model calculation of Scherer and Barjhoux[14] (and to indicate a discrepancy between their results and ours) as well as to present an explanation of the magnetic ordering in $CsNiF_3$ from a different and

clearer point of view.

The polarization vector in (3.3) can be written in the general form.

$$S=\mathbf{S}_1+i\mathbf{S}_2 , \tag{3.12}$$

where $\mathbf{S}_1$ and $\mathbf{S}_2$ are real vectors, and the spin density modulation becomes

$$\rho(\mathbf{r})=2[\mathbf{S}_1\cos(\mathbf{Q}\cdot\mathbf{r})-\mathbf{S}_2\sin(\mathbf{Q}\cdot\mathbf{r})] . \tag{3.13}$$

The Kronecker δ function involving $\mathbf{Q}$ in the free energy (3.4) requires that the two cases $\mathbf{Q}\neq\frac{1}{2}\mathbf{G}_1$ and $\mathbf{Q}=\frac{1}{2}\mathbf{G}_1$ be considered separately. For $\mathbf{Q}\neq\frac{1}{2}\mathbf{G}_1$, the analysis of fourth-order (in S) contributions to the free energy shows that a helical polarization, described by $\mathbf{S}_1\perp\mathbf{S}_2$ and $|\mathbf{S}_1|=|\mathbf{S}_2|\equiv S/2^{1/2}$ is stabilized. For $\mathbf{Q}=\frac{1}{2}\mathbf{G}$, contributions to the spin density (3.2) and (3.13) involving $\mathbf{S}_2$ are zero since $\mathbf{R}\cdot\mathbf{G}_1=2\pi n$ for hexagonal crystals. The spin density for this case can thus also be chosen to have a helical polarization without loss of generality, which simplifies the analysis below. It remains to be shown what values of $\mathbf{Q}$ and which orientation of $\mathbf{S}_1$ (with respect to the crystallographic axes) minimize $F_S^{(2)}$.

With $\mathbf{S}$ given by (3.12) for a helical polarization and θ the angle (measured clockwise) between $\mathbf{S}_1$ and $\hat{\mathbf{x}}$ (see Fig. 1), the second-order contributions to the free energy can be expressed by (see 3.4).

$$F_S^{(2)}=A_{\mathbf{Q}}S^2 , \tag{3.14}$$

where

$$A_{\mathbf{Q}}(\theta)=J_{\mathbf{Q}}+D_{\mathbf{Q}}+D_{z\mathbf{Q}}+\tfrac{1}{2}(d_{\mathbf{Q}}^{xx}+d_{\mathbf{Q}}^{yy}) +\tfrac{1}{2}[(d_Q^{xx}-d_Q^{yy})\cos(2\theta)-2d_Q^{xy}\sin(2\theta)]\Delta_{2\mathbf{Q},\mathbf{G}_1} . \tag{3.15}$$

With only nearest-neighbor interactions included in the basal plane, $J_{\mathbf{Q}}$ is given by (3.8) and (3.9), and $D_{\mathbf{Q}}$, $D_{z\mathbf{Q}}$, and $d_{\mathbf{Q}}^{\alpha\beta}$, derived from (3.10) and (3.11), are given by

$$\begin{aligned} &D_{\mathbf{Q}}+D_{z\mathbf{Q}}=D_c+2D_1f(x,y) ,\\ &d_{\mathbf{Q}}^{xx}=d_1[2\cos(x)+\cos(\tfrac{1}{2}x)\cos(y)] ,\\ &d_{\mathbf{Q}}^{yy}=3d_1\cos(\tfrac{1}{2}x)\cos(y) ,\\ &d_{\mathbf{Q}}^{xy}=-3^{1/2}d_1\sin(\tfrac{1}{2}x)\sin(y) , \end{aligned} \tag{3.16}$$

where

$$D_1=\tilde{D}(a)+\tilde{D}_z(a),\quad d_1=\tilde{d}(a) .$$

For wave vectors $\mathbf{Q}\neq\frac{1}{2}\mathbf{G}_1$, $F_s^{(2)}$ is independent of θ and $f(x,y)$ is minimized with

$$\mathbf{Q}_1=\frac{4\pi}{3a}\hat{\mathbf{x}} \text{ or } \mathbf{Q}_2=\frac{2\pi}{3a}\hat{\mathbf{x}}+\frac{\pi}{b}\hat{\mathbf{y}} \text{ if } (2J_a+2D_1+d_1)>0 ,$$

which gives the 120° spin structure shown in Fig. 2. A planar ferromagnetic structure $Q=0$ is realized if $(2J_a+2D_1+d_1)<0$. The free energy $F_s^{(2)}$ is the same for both $\mathbf{Q}_1$ and $\mathbf{Q}_2$ and is given by

$$F_s^{(2)}(120°)=[2J_c+D_c-3(J_a+D_1+\tfrac{1}{2}d_1)]S^2 , \tag{3.17}$$

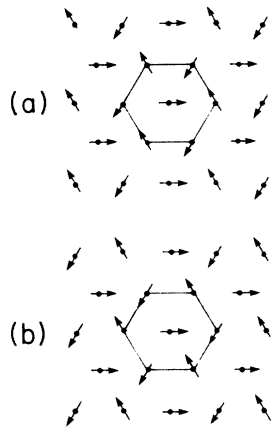

FIG. 2. Two-domain 120° spin structure predicted by the theory for weak-dipole-like coupling (also see Ref. 14) where for (a) $\mathbf{Q}_1=4\pi/(3a)\hat{\mathbf{x}}$, (b) $\mathbf{Q}_2=2\pi/(3a)\hat{\mathbf{x}}+\pi/b\hat{\mathbf{y}}$.

so that a two-domain structure is predicted for this case. Spin structures characterized by wave vectors $\mathbf{Q}_1$ and $\mathbf{Q}_2$ have been observed in $CsNiCl_3$ (see Ref. 7) and $RbFeCl_3$ (see Ref. 8). For the case of $RbFeCl_3$, the spins form the 120° structure at low temperatures. Note that this analysis also applies to the case where $d=0$, e.g., in the absence of dipole interactions of the models of Refs. 14 and 15. The free energy for the 120° structure is independent of the angle θ if terms up to fourth order is S are included. Planar hexagonal anisotropy enters at sixth order[7] and is of the form $F_C=CS^6\cos6\theta$. This term is minimized with $\theta=0°$, 60°, 120° for $C<0$, so that the choice of moment alignment shown in Fig. 2 can be realized.

For wave vectors $\mathbf{Q}=\frac{1}{2}\mathbf{G}_1$, three nonequivalent choices can be made from (3.7)

$$\mathbf{Q}_a=\frac{\pi}{b}\hat{\mathbf{y}},\quad \mathbf{Q}_b=\frac{\pi}{a}\hat{\mathbf{x}}+\frac{\pi}{2b}\hat{\mathbf{y}},\quad \mathbf{Q}_c=\frac{\pi}{a}\hat{\mathbf{x}}-\frac{\pi}{2b}\hat{\mathbf{y}} . \tag{3.18}$$

For each of these wave vectors it is necessary to minimize the free energy with respect to θ. The results are $\theta_a=0°$, $\theta_b=60°$, $\theta_c=120°$ for the case where $d_1<0$. For each case $\mathbf{S}_1\perp\mathbf{Q}$. The observed three-domain antiferromagnetic ordering of $CsNiF_3$ shown in Fig. 1 is described by these values of $\mathbf{Q}$ and θ. It is reasonable to expect that d_1 is negative since the main contribution to the terms d in the free energy (3.1) arises from magnetic dipole interactions. The free energy for each of the three structures is the same, given by

$$F_S^{(2)}(AF)=[2J_c+D_c-2(J_a+D_1-\tfrac{1}{2}d_1)]S^2 . \tag{3.19}$$

From the analysis given above and a comparison of the free energies (3.17) and (3.19), the following conclusions can be made. With the parameter j defined by

$$j=J_a+D_1+\tfrac{1}{2}d_1 \tag{3.20}$$

we have found that the ferromagnetic state is realized for $j<0$, the antiferromagnetic state for $0<j<2|d_1|$, and

the 120° state for $j > 2|d_1|$. Corresponding expressions which result from including up to third-neighbor interactions are given in the Appendix.

It is of interest to compare these results with the Heisenberg-dipole models of Scherer and Barjhoux[14] and Suzuki.[15] This is achieved by setting $D(\mathbf{R})=\gamma_D/R^5$, $d(\mathbf{R})=-3D(\mathbf{R})$, and $D_z(\mathbf{R})=0$, where γ_D is the dipole strength. The c-axis sums in (3.11) can then be evaluated with a knowledge of c/a. Using the numerically determined result $d_1 \simeq -2D_1$, so that $j \simeq J_a$, the possible ordered states that are realized from this model are as follows: ferromagnetic $(J_a/\gamma_D)<\alpha_1$, antiferromagnetic $\alpha_1<(J_a/\gamma_D)<\alpha_2$, 120° structure $(J_a/\gamma_D)>\alpha_2$, where $\alpha_1 \simeq 0$, $\alpha_2 \simeq 19.1$ if only first-neighbor interactions are included, and $\alpha_1 \simeq 0$, $\alpha_2 \simeq 12.7$ when up to third-neighbor interactions (see the Appendix) are accounted for. These results corroborate the conclusions of Suzuki[15] where $\alpha_1 \simeq 0.4$ and $\alpha_2 \simeq 14.2$ if a large number of neighbor interactions are included. Our conclusions differ, however, from those of Scherer and Barjhoux[14] who find from their nearest-neighbor model that the antiferromagnetic state is realized for $-2.4<(J_a/\gamma_D)<4.8$ and the 120° state occurs only for $(J_a/\gamma_D)\gg 1$. This discrepancy is puzzling since their model contains the same essential ingredients as ours.

From a variety of experimental data on $CsNiF_3$, Scherer and Barjhoux[14] have estimated that $(J_a/\gamma_D)\simeq 3.3$ and Suzuki[15] uses the value 2.3. The antiferromagnetic ordering shown in Fig. 1 is thus predicted to occur for all of the dipole models discussed here. We emphasize that the phenomenological free energy developed in this work accounts for all types of microscopic interactions allowed by symmetry and is not restricted to the dipole model.

C. Fourth-order terms

The influence of contributions to the free energy of order s^4 on the types of magnetic ordering which can occur in $CsNiF_3$ is examined here. Using (3.2), (3.3), and (3.6), the term of order s^4 in the free energy (3.1) can be evaluated with the result

$$F_s^{(4)}=B_1(\mathbf{S}\cdot\mathbf{S}^*)^2+\tfrac{1}{2}B_2|\mathbf{S}\cdot\mathbf{S}|^2 + \tfrac{1}{4}B_3[(\mathbf{S}\cdot\mathbf{S})^2+(\mathbf{S}^*\cdot\mathbf{S}^*)^2]\Delta_{4\mathbf{Q},\mathbf{G}_1} + B_4(\mathbf{S}\cdot\mathbf{S}^*)[\mathbf{S}\cdot\mathbf{S}+\mathbf{S}^*\cdot\mathbf{S}^*]\Delta_{2\mathbf{Q},\mathbf{G}_1}\,, \tag{3.21}$$

where

$$\begin{aligned} B_1&=B_{\mathbf{Q},-\mathbf{Q},\mathbf{Q},-\mathbf{Q}}\,,\\ B_2&=B_{\mathbf{Q},\mathbf{Q},-\mathbf{Q},-\mathbf{Q}}\,,\\ B_3&=B_{\mathbf{Q},\mathbf{Q},\mathbf{Q},\mathbf{Q}}\,,\\ B_4&=B_{-\mathbf{Q},\mathbf{Q},\mathbf{Q},\mathbf{Q}}\,, \end{aligned} \tag{3.22}$$

with

$$B_{\mathbf{q}_1,\mathbf{q}_2,\mathbf{q}_3,\mathbf{q}_4}=\Delta_{\mathbf{q}_1+\mathbf{q}_2+\mathbf{q}_3+\mathbf{q}_4,\mathbf{G}}\left[\frac{V}{N}\right]^3\sum_{\mathbf{R}_1\mathbf{R}_2\mathbf{R}_3}B(\mathbf{R}_1,\mathbf{R}_2,\mathbf{R}_3)e^{i(\mathbf{q}_1\cdot\mathbf{R}_1+\mathbf{q}_2\cdot\mathbf{R}_2+\mathbf{q}_3\cdot\mathbf{R}_3)}\,, \tag{3.23}$$

where $\mathbf{G}$ is a reciprocal lattice vector and $\mathbf{R}_i$ are lattice vectors. In deriving these results, inversion symmetry has been used as well as the dependence of $B\{\mathbf{r}_i\}$ on differences between pairs of coordinates only so that, e.g.,

$$B(\mathbf{r}_1,\mathbf{r}_2,\mathbf{r}_3,\mathbf{r}_4)=B(\mathbf{r}_1-\mathbf{r}_4,\mathbf{r}_2-\mathbf{r}_4,\mathbf{r}_3-\mathbf{r}_4)\,.$$

Consider first the case where $4\mathbf{Q}\neq\mathbf{G}_1$ and $2\mathbf{Q}\neq\mathbf{G}_1$, so that the last two terms of (3.21) are zero. The sign of the coefficient B_2 then determines the type of polarization $\mathbf{S}$, which minimizes the free energy.[18] It is straightforward to show that a linearly polarized state (where $\mathbf{S}$ can be taken as real) is stabilized if $B_2<0$ and $(B_1+\frac{1}{2}B_2)>0$ whereas a helical polarization ($\mathbf{S}\cdot\mathbf{S}=0$) is favored if $B_2>0$ and $B_1>0$. The coefficients B_1 and B_2 differ due to the wave-vector dependence of $B_{\{\mathbf{q}_i\}}$. For $CsNiF_3$, where $\mathbf{Q}$ lies in the basal plane and there are strong exchange interactions along the c axis with only weak-interchain coupling, it can thus be assumed that the wave-vector dependence of this coefficient is weak [in a manner similar to $A_{\mathbf{Q}}$ (3.15)]. Since B_1 must be positive for stability, it is then reasonable to assume that B_2 is also positive and the helical polarization is realized. Similar conclusions can be made for the case where $4\mathbf{Q}=\mathbf{G}_1$, so that $B_3>0$ also serves to stabilize the helical state.

It is not necessary to use the weak-$\mathbf{Q}$ dependence of B for the case where $2\mathbf{Q}=\mathbf{G}_1$. This is due to the fact that $B_{\{\mathbf{q}_i+\mathbf{G}_i\}}=B_{\{\mathbf{q}_i\}}$, where $\mathbf{G}_i$ are reciprocal lattice vectors, so that $-\mathbf{Q}=\mathbf{Q}+\mathbf{G}_1$ can be used to show $B_1=B_2=B_3=B_4$ from Eqs. (3.22). Stability requires that $B_i>0$, so it would appear that the helical polarization is preferred and

$$F_s^{(4)}=\tfrac{1}{2}BS^4\,, \tag{3.24}$$

where $B=2B_i$. In fact, a linear polarization has the same total free energy if $2\mathbf{Q}=\mathbf{G}_1$ since for this case the second-order contributions appear as $2A_{\mathbf{Q}}S^2$ [see (3.15)] and the fourth-order terms are $2BS^4$ and minimization yields $S_{\text{lin}}^2=\frac{1}{2}S_{\text{hel}}^2$, $F_{\text{lin}}=F_{\text{hel}}$. This must be the case since, as discussed after (3.13), the spin configuration (3.2) and (3.3) is the same for helical and linear polarizations if $2\mathbf{Q}=\mathbf{G}_1$. We emphasize that the equality of the fourth-order coefficients B_i for $CsNiF_3$ is a consequence of the fact that $\mathbf{Q}=\frac{1}{2}\mathbf{G}_1$. For systems with other types of ordering (apart from $Q=0$) the B_i are *a priori* unrelated, which can lead to some important consequences (see Refs. 18 and 30).

Despite the result that fourth-order terms are minimized by a helical polarization of the spin vector, the possibility exists that second-order terms could lower the free energy sufficiently with a linear polarization such that $F_{\rm lin} < F_{\rm hel}$ for $\mathbf{Q} \neq \frac{1}{2}\mathbf{G}_1$. This has been explored in detail in Ref. 15, where for the case of weak-dipole coupling (e.g., $RbFeCl_3$) incommensurate sinusoidal phases can be realized. For $CsNiF_3$, where the dipole interaction is relatively strong, the possibility for the occurrence of an incommensurate sinusoidal phase in the presence of an applied magnetic field along the x axis was found.[15] There is no experimental evidence to support the existence of such a phase in this material,[13] and this possibility will not be explored further here. We emphasize, however, that these incommensurate states can be realized using the free energy developed in this work.

IV. MAGNETIC FIELD EFFECTS

A. H in the basal plane

An important effect of applying a magnetic field in the basal plane perpendicular to one of the moment directions of the domains in Fig. 1 is to force a single-magnetic-domain state. For a field applied along a direction $\hat{\mathbf{y}}$, $\frac{1}{2}(3^{1/2}\hat{\mathbf{x}}+\hat{\mathbf{y}})$ or $\frac{1}{2}(3^{1/2}\hat{\mathbf{x}}-\hat{\mathbf{y}})$, the crystal will consist mainly of a spin ordering as shown in Fig. 1(a), 1(b), or 1(c), respectively, for field strengths greater than about 500 Oe.[13] Domain-size effects will not be analyzed here, and it will be assumed that the crystal is in a single-domains state (except for the special case where $\mathbf{H} \| \hat{\mathbf{x}}$ discussed below).

An applied magnetic field also induces a homogeneous component of the magnetization $\mathbf{m}$, so that [see (3.3)] the vector $\boldsymbol{\rho}(\mathbf{r})$ is now expressed by

$$\boldsymbol{\rho}(\mathbf{r}) = \mathbf{m} + \mathbf{S}e^{i\mathbf{Q}\cdot\mathbf{r}} + \mathbf{S}^* e^{-i\mathbf{Q}\cdot\mathbf{r}} . \tag{4.1}$$

Using (4.1) in (3.1) with a Zeeman term added, results in the following free energy appropriate for an analysis of effects induced by applying a field in the basal plane of $CsNiF_3$

$$F = A_{\mathbf{Q}} S^2 + \tfrac{1}{2} B S^4 + \tfrac{1}{2} A_0 m^2 + \tfrac{1}{8} B m^4 + B(\mathbf{m}\cdot\hat{\mathbf{S}}_1)^2 S^2 + \tfrac{1}{2} B m^2 S^2 - \mathbf{m}\cdot\mathbf{H} , \tag{4.2}$$

where $A_{\mathbf{Q}}$ is given by (3.15), $A_0 = A_{Q=0}$, and $\hat{\mathbf{S}}_1$ gives the direction of the long-range ordered part of the spin density [see (3.13)]. Note that this result is based on the assumption that the coefficient $B_{\{\mathbf{q}_i\}}$ given by (3.23) is nearly wave-vector independent.

The term involving $\hat{\mathbf{S}}_1$ is minimized for $\mathbf{m} \perp \hat{\mathbf{S}}_1$ since $B > 0$, and the Zeeman term lowers the free energy for $\mathbf{m} \| \mathbf{H}$. A domain with $\mathbf{S}_1$ perpendicular to $\mathbf{H}$ is thus seen to be energetically favorable. Using numerical estimates of relevant parameters, it is argued below that $Bm^2S^2 \ll mH$ so that $\mathbf{m}$ will be nearly parallel to $\mathbf{H}$ even for cases where $\mathbf{H}$ is not perpendicular to $\mathbf{S}_1$. For some field directions there may be an induced rotation of $\mathbf{S}_1$, as well as domain-size changes.

Minimization of the free energy (4.2) for the single-domain case with $\mathbf{m} \| \mathbf{H}$ and $\mathbf{S}_1 \perp \mathbf{m}$ leads to the following results.[20] There is a critical field H_c, where for $H > H_c$ $S^2 = 0$, given by

$$H_c^2 = 2\chi^{-2} B^{-1} a (T_{N0} - T) , \tag{4.3}$$

where

$$\chi^{-1} = A_0 - A_{\mathbf{Q}} , \tag{4.4}$$

and $A_{\mathbf{Q}} \equiv a(T - T_{N0})$, with T_{N0} being the transition temperature in zero field. It is assumed here that χ is independent of temperature. For $H > H_c$ the magnetization is given by

$$A_0 m + \tfrac{1}{2} B m^3 = H \tag{4.5}$$

and for $H < H_c$

$$m = \chi H , \tag{4.6}$$

$$S^2 = \tfrac{1}{2}\chi(H_c^2 - H^2) . \tag{4.7}$$

Numerical estimates of the parameters a, B, and χ can be obtained by a comparison of the above expressions with available data on $m(H)$, $H_c(T)$ as well as an analysis of the specific heat anomaly at T_N. All parameters will be given in cgs units. Unfortunately there is no published data for $m(H)$ at temperatures below T_{N0}. A crude estimate of χ can be obtained using measured results[21] for the magnetization at $T \gtrsim T_{N0}$ and small field strengths. For this case, the term Bm^3 in (4.5) is assumed to be small and since $A_{\mathbf{Q}}$ is also small, $A_0 \simeq \chi^{-1}$ so that $m \simeq \chi H$. The curve for $m(H)/m_s$ at $T = 2.65$ K (Fig. 2 of Ref. 21) is nearly linear for fields $H \lesssim 1$ kOe. Using a value for the saturation magnetization $m_S = g\mu_B N/V \simeq 240$ emu/cm^3 (with g taken[21,22] to be 2.3) the estimate $\chi^{-1} \simeq 0.13$ is obtained.

Using this value of χ, a/B can be estimated by a comparison of $H_c(T)$ (4.3) with corresponding data from Ref. 13. The results shown in Fig. 3, with $a/B = 7.5 \times 10^4$, where obtained by fitting the expression for $H_c(T)$ to the data close to T_{N0} (here taken to be 2.7 K). Note that the mean-field theory above predicts $H_c(T) \propto S_0(T)$, where

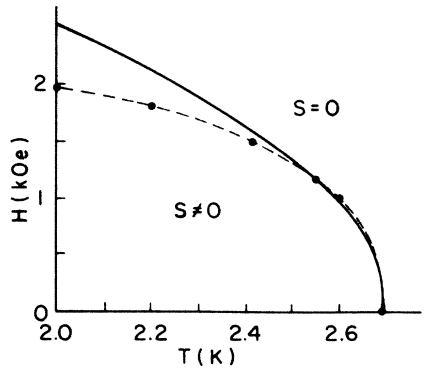

FIG. 3. Magnetic phase diagram for $CsNiF_3$ with $\mathbf{H}$ in the basal plane. Circles (with broken line) are from the data of Ref. 13 and the solid line from the fitted theory (4.3).

$S_0(T)$ is the zero-field expression for the amplitude of the magnetic order. The good agreement between theory and experimental data shown in Fig. 3 for 2.45 K $< T < T_{N0}$ is thus expected[12] (see remarks in the Introduction).

The free energy (4.2) can also be used to obtain an expression for the specific-heat anomaly at $T=T_{N0}$. The mean-field theory predicts a discontinuity (at constant stress) given by (also see Ref. 23)

$$\Delta C = C^+ - C^- = -T_{N0}a^2/B \tag{4.8}$$

in zero field where $C^{+/-}=C(T\rightarrow T_{N0}^{+/-})$. An estimate of $\Delta C \simeq -8.7\times 10^4$ erg/(K-cm^3) can be extrapolated from the data of Ref. 17. Using this result and (4.8) (with $T_{N0}=2.65$ K) along with the above estimate for a/B gives $a\simeq 0.44$ and $B\simeq 5.9\times 10^{-6}$. We emphasize that these values may be little more than order-of-magnitude estimates.

The above parameter estimates can be used to determine the relative size of the terms $F_1=B(\mathbf{m}\cdot\hat{\mathbf{S}}_1)^2S^2$ and $F_2=\mathbf{m}\cdot\mathbf{H}$ in the free energy (4.2). With the assumption that $\mathbf{m}$ is nearly parallel to $\mathbf{H}$, using $S^2 \lesssim |A_Q|/B$ and (4.6), the relation

$$F_1/F_2 \lesssim \chi a(T-T_{N0}) \simeq 0.06(T-T_{N0})$$

so that $F_1 \ll F_2$ in a temperature range not too far from T_{N0}. This analysis justifies the assumption that $\mathbf{m}$ is nearly parallel to $\mathbf{H}$.

Yamazaki *et al.*[24] have proposed the two-domain spin ordering shown in Fig. 4 for the case where $\mathbf{H}\|\hat{\mathbf{x}}$ and $|\mathbf{H}| \lesssim |\mathbf{H}_c|$ (also see Ref. 15). These magnetically-ordered domains can be obtained from the structures shown in Figs. 1(b) and 1(c) by a rotation of the magnetic moments. Such a state is shown here to be a consequence of an analysis of the free energy discussed in Sec. II B and the magnetic-field effects discussed above.

For $\mathbf{H}\|\hat{\mathbf{x}}$, it is assumed that as the field increases from zero, domain (*a*) of Fig. 1 decreases in size as it is the most energetically unfavorable due to the term $B(\mathbf{m}\cdot\mathbf{S}_1)^2S^2$ in (4.2). This term also causes the moments in domains (*b*) and (*c*) of Fig. 1 to rotate towards a configuration, where $\mathbf{S}_1$ is perpendicular to $\mathbf{m}$ (and $\mathbf{H}$) until the state shown in Fig. 4 is achieved. Putting $\theta=90°$ in the expression (3.14) for $F_S^{(2)}$ shows that the free energy is then minimized by the wave vectors $\mathbf{Q}_b$ and $\mathbf{Q}_c$ of

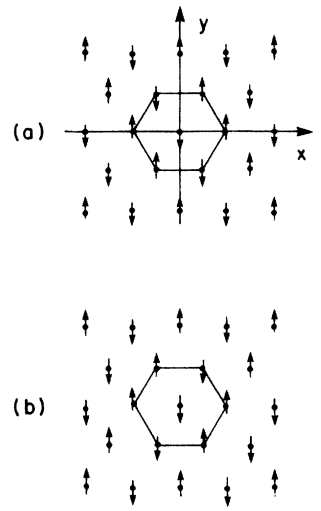

FIG. 4. Two-domain state for $\mathbf{H}\|\hat{\mathbf{x}}$ proposed by Yamazaki *et al.* (Ref. 24).

(3.18), so that $F_s^{(2)}=A_Q(90°)S^2$, where (with only nearest-neighbor interactions included)

$$A_Q(90°)=2J_c+D_c-2J_a-2D_1 \tag{4.9}$$

to be compared with $A_Q(\theta)$ for $\theta=60°$, 120° given by (3.14) and (3.19). A detailed analysis of the θ dependence of the full free energy (4.2) reveals that the configuration shown in Fig. 4 is realized only for $H\rightarrow H_{cx}$, where $S^2=0$ for $H>H_{cx}$ and

$$H_{cx}^2=2\chi^{-2}B^{-1}|A_Q(90°)|=H_c^2+2\chi^{-2}B^{-1}d_1 . \tag{4.10}$$

This result shows that $H_{cx} \lesssim H_c$ [where H_c is the critical field (4.3) for $\mathbf{H}$ perpendicular to one of the spin domains of Fig. 1] since d_1 is assumed to be negative, in agreement with Ref. 24.

B. H parallel to ĉ

Additional contributions to the free energy (3.1) for the case where $\mathbf{s}(\mathbf{r})$ has a nonzero $\hat{\mathbf{z}}$ component can be obtained from the general expression (2.2). For hexagonal symmetry, these terms are

$$\begin{aligned}F_z=&\frac{1}{2V}\int d\mathbf{r}\,d\mathbf{r}'\,J_z(\tau)s_z(\mathbf{r})s_z(\mathbf{r}')\\&+\frac{1}{2V}\int d\mathbf{r}\,d\mathbf{r}'[D_{1z}(\tau)\tau^2+D_{2z}(\tau)\tau_z^2]s_z(\mathbf{r})s_z(\mathbf{r}')+\frac{1}{2V}\int d\mathbf{r}\,d\mathbf{r}'\,d_3(\tau)\tau_z s_z(\mathbf{r})[\tau_x s_x(\mathbf{r}')+\tau_y s_y(\mathbf{r}')]\\&+\frac{1}{4V}\int d\mathbf{r}_1\,d\mathbf{r}_2\,d\mathbf{r}_3\,d\mathbf{r}_4(E_1\{\mathbf{r}_i\}[s_x(\mathbf{r}_1)s_x(\mathbf{r}_2)+s_y(\mathbf{r}_1)s_y(\mathbf{r}_2)]s_z(\mathbf{r}_3)s_z(\mathbf{r}_4)+E_2\{\mathbf{r}_i\}s_z(\mathbf{r}_1)s_z(\mathbf{r}_2)s_z(\mathbf{r}_3)s_z(\mathbf{r}_4)) ,\end{aligned} \tag{4.11}$$

where $\tau=\mathbf{r}-\mathbf{r}'$ and E_1, E_2 depend only on differences between pairs of coordinates $\mathbf{r}_1\rightarrow\mathbf{r}_4$. Supported by the analysis of Sec. IV A, it is assumed here that for $\mathbf{H}\|\hat{\mathbf{z}}$ the spin ordering is described by $\rho(\mathbf{r})$ (4.1) with $\mathbf{m}\|\hat{\mathbf{z}}$ and the three-domain structure of Fig. 1. This spin structure yields the following contributions to F_z:

$$F_z=\tfrac{1}{2}A_{z0}m_z^2+\tfrac{1}{2}E_1m_z^2S^2+\tfrac{1}{4}E_2m_z^4 , \tag{4.12}$$

where

$$A_{z0}=\frac{V}{N}\sum_{\mathbf{R}}[J_z(\mathbf{R})+D_{1z}(\mathbf{R})R^2 + D_{2z}(\mathbf{R})R_z^2+d_3(\mathbf{R})(R_x+R_y)R_z] \quad (4.13)$$

and

$$E_1=E_{1\mathbf{Q},-\mathbf{Q},0,0},\quad E_2=E_{20,0,0,0}$$

with $E_{\{\mathbf{q}_i\}}$ defined similar to $B_{\{\mathbf{q}_i\}}$ given by (3.23).

Adding to the free energy (4.2), with $\mathbf{m}\perp\mathbf{S}_1$ and $\mathbf{m}\parallel\mathbf{H}$, gives

$$F=A_{\mathbf{Q}}S^2+\tfrac{1}{2}BS^4+\tfrac{1}{2}(A_0+A_{z0})m^2 + \tfrac{1}{2}\tilde{B}_1m^2S^2+\tfrac{1}{8}\tilde{B}_2m^4-m\mathbf{H}\ , \quad (4.14)$$

where

$$\tilde{B}_1=B+E_1,\quad \tilde{B}_2=B+2E_2\ . \quad (4.15)$$

Minimization of (4.14) with respect to S^2 and m gives the following results. The critical field H_{cz} above which $S^2=0$ is given by

$$H_{cz}^2=2a(T_{N0}-T)\tilde{B}_1^{-1}(\chi^{-1}+A_{z0}-bA_{\mathbf{Q}})^2\ , \quad (4.16)$$

where χ is given by (4.4) and $b=(2E_2-E_1)/\tilde{B}_1$. The magnetization m for $H>H_{cz}$ satisfies the equation

$$(A_0+A_{z0})m+\tfrac{1}{2}\tilde{B}_2m^3=H \quad (4.17)$$

and for $H<H_{cz}$, it is the solution of

$$(\chi^{-1}+A_{z0}-b_1A_{\mathbf{Q}})m+\tfrac{1}{2}(2b_2-2b_1-b_1^2)Bm^3=H\ , \quad (4.18)$$

where $b_i=E_i/B$.

It is known[11] that the coefficient corresponding to A_{z0} in a Heisenberg-type Hamiltonian is very large for $CsNiF_3$, and it is reasonable to expect the magnetization will be dominated by these terms in (4.17) and (4.18), at least for low fields. With this assumption,

$$m\simeq\chi_zH,\quad \chi_z^{-1}=A_{z0} \quad (4.19)$$

for both $H>H_{cz}$ and $H<H_{cz}$. The magnetization data for $\mathbf{H}\parallel\hat{\mathbf{z}}$ of Ref. 21 (at $T>T_{N0}$) shows that $m(H)$ indeed varies linearly with field, with a very small temperature dependence of the slope for $T\gtrsim T_{N0}$. A comparison of these results with (4.19) gives the estimate $\chi_z\simeq5\times10^{-3}$ or $A_{z0}\simeq200$. This justifies the assumption that $A_{z0}\gg\chi^{-1}$, $b_iA_{\mathbf{Q}}$, and the critical field can thus be approximated by

$$H_{cz}^2\simeq2A_{z0}^2\tilde{B}_1^{-1}a(T_{N0}-T)\ . \quad (4.20)$$

It can be expected that $\tilde{B}_1$ is of the same order in magnitude as B, so that the estimate $H_{cz}/H_c\sim25$, from (4.3) and (4.20), can be made.

V. MAGNETOELASTIC COUPLING

Interactions between the long-range magnetic ordering below T_N in $CsNiF_3$ and the lattice are investigated here within the framework of the phenomenological free energy presented in Sec. II. The fact that a number of different magnetic orientations can be achieved by the application of a small magnetic field provides for some interesting consequences of the model which can be examined experimentally. Magnetoelastic contributions to the free energy invariant under hexagonal symmetry which account for uniform strain-spin coupling are given in Sec. V A. Explicit expressions for the behavior of thermal expansion and the elastic constants at $T\simeq T_N$ are presented in Sec. V B. In Sec. V C, the effects of applying uniaxial stress on the magnetic domains as well as the Néel temperature are considered. Dilation of the lattice in response to an applied magnetic field (magnetostriction) is considered in Sec. V D and the possibility of magnetization induced inhomogeneous strain is investigated in Sec. V E.

A. Hexagonal symmetry and uniform strain

Magnetoelastic coupling contributions to the free energy (2.3), invariant with respect to hexagonal symmetry, which involve the uniform part of the strain tensor (2.5) can be expressed as

$$F_{se}=\frac{1}{2V}\int d\mathbf{r}\,d\mathbf{r}'([K_1(\tau)(e_{xx}+e_{yy})+K_3(\tau)e_{zz}]\mathbf{s}(\mathbf{r})\cdot\mathbf{s}(\mathbf{r}')+k(\tau)\{e_{xx}s_y(\mathbf{r})s_y(\mathbf{r}')+e_{yy}s_x(\mathbf{r})s_x(\mathbf{r}') - e_{xy}[s_x(\mathbf{r})s_y(\mathbf{r}')+s_x(\mathbf{r}')s_y(\mathbf{r})]\})\ , \quad (5.1)$$

where it has been assumed $\mathbf{s}(\mathbf{r})$ lies in the basal plane. Using $\mathbf{s}(\mathbf{r})$ given by (3.2) and (3.3) along with the assumption that the long-range magnetic order can be described as in Sec. II by $\mathbf{Q}=\frac{1}{2}\mathbf{G}_1$ as well as the angle θ which gives the orientation of the moments, (5.1) can be reduced to

$$F_{se}=K_1(e_{xx}+e_{yy})S^2+K_3e_{zz}S^2 + k[e_{xx}\sin^2\theta+e_{yy}\cos^2\theta-e_{xy}\sin(2\theta)]S^2\ , \quad (5.2)$$

where

$$K_j=K_{j\mathbf{Q}}=\frac{V}{N}\sum_{\mathbf{R}}K_j(\mathbf{R})e^{i\mathbf{Q}\cdot\mathbf{R}}\ , \quad (5.3)$$

$$k=k_{\mathbf{Q}}=\frac{V}{N}\sum_{\mathbf{R}}k(\mathbf{R})e^{i\mathbf{Q}\cdot\mathbf{R}}\ . \quad (5.4)$$

All domain (spin) orientation effects are contained in the k term, which is expected to be small since k arises from spin-orbit coupling effects and K_i are due to exchange interactions. It is also convenient to express (5.2) in the

form

$$F_{se}=\tilde{K}_i e_i S^2 \tag{5.5}$$

in the Voigt notation, where

$$\tilde{K}_1=K_1+k\sin^2\theta,\quad \tilde{K}_2=K_1+k\cos^2\theta,\quad \tilde{K}_3=K_3$$
$$\tilde{K}_4=\tilde{K}_5=0,\quad \tilde{K}_6=\tfrac{1}{2}k\sin(2\theta)\ . \tag{5.6}$$

B. Thermal expansion and the elastic constants

The change in the strain tensor induced by the onset of long-range magnetic order is determined by minimizing the free energy with respect to e_i, with the result

$$e_i=-s_{ij}\tilde{K}_j S^2\ , \tag{5.7}$$

where s_{ij} is the compliance matrix, $s_{ij}=(\overleftrightarrow{C}^{-1})_{ij}$, appropriate for hexagonal symmetry. Using the results from Sec. IV that $S^2=0$ for $T>T_{N0}$ and $S^2=a(T_{N0}-T)/B$ for $T<T_{N0}$, this mean-field theory is thus seen to predict a change in slope of the thermal expansion at $T=T_{N0}$. The discontinuity in the thermal expansion coefficient $\Delta\alpha_i=\alpha_i^+-\alpha_i^-$, where $\alpha_i=\partial e_i/\partial T$, is thus given by (also see Ref. 23)

$$\Delta\alpha_i=-aB^{-1}s_{ij}\tilde{K}_j\ . \tag{5.8}$$

Using the expressions for $\tilde{K}_i$ (5.6), the components of the thermal-expansion discontinuity are

$$\begin{aligned}
\Delta\alpha_{xx}&=-aB^{-1}[(K_1+k\sin^2\theta)s_{11}\\
&\qquad+(K_1+k\cos^2\theta)s_{12}+K_3s_{13}]\\
\Delta\alpha_{yy}&=-aB^{-1}[(K_1+k\cos^2\theta)s_{11}\\
&\qquad+(K_1+k\sin^2\theta)s_{12}+K_3s_{13}]\\
\Delta\alpha_{zz}&=-aB^{-1}[2\bar{K}s_{13}+K_3s_{33}]\\
\Delta\alpha_{xy}&=-\tfrac{1}{2}aB^{-1}k\sin(2\theta)s_{66}
\end{aligned} \tag{5.9}$$

where $\alpha_6=2\alpha_{xy}$ has been used and

$$\bar{K}=K_1+\tfrac{1}{2}k\ . \tag{5.10}$$

Note that the theory predicts no change for α_{xz} and α_{yz}.

In the absence of an applied magnetic field (or uniaxial stress), the crystal will magnetically order to the three-domain state shown in Fig. 1. The appropriate thermal-expansion discontinuities are obtained by averaging the results (5.9) over the three orientations of the spin $\theta_a=0°$, $\theta_b=60°$, and $\theta_c=120°$ with the result

$$\overline{\Delta\alpha}_{xx}=\overline{\Delta\alpha}_{yy}=-aB^{-1}[\bar{K}(s_{11}+s_{12})+K_3s_{13}] \tag{5.11}$$

along with $\overline{\Delta\alpha}_{zz}=\Delta\alpha_{zz}$ (5.9) and $\overline{\Delta\alpha}_{xy}=0$.

Only a small magnetic field of ~ 500 Oe is required to achieve a nearly single-domain crystal,[13] and the zero-field results given by (5.9) remain valid for low field strengths (see Sec. V D). If such a small field is applied along $\hat{\mathbf{y}}$, the crystal will be in the domain-(a) state so that, with $\theta=0$, a prediction of the model is

$$\begin{aligned}
\Delta\alpha_{xx}^{(a)}&=-aB^{-1}[K_1(s_{11}+s_{12})+K_3s_{13}]\ ,\\
\Delta\alpha_{yy}^{(a)}&=\Delta\alpha_{xx}^{(a)}-aB^{-1}k(s_{11}-s_{12})\ ,
\end{aligned} \tag{5.12}$$

and $\Delta\alpha_{xy}^{(a)}=0$.

The free energy can also be used to obtain expressions for the mean-field-type discontinuity in the adiabatic elastic constants (also see Ref. 23) at T_N:

$$\Delta C_{ij}=C_{ij}^+-C_{ij}^-=\tilde{K}_i\tilde{K}_j/B\ . \tag{5.13}$$

Using (5.6), the nonzero components of ΔC_{ij} are given by (with $\Delta C_{ji}=\Delta C_{ij}$)

$$\begin{aligned}
\Delta C_{11}&=(K_1+k\sin^2\theta)^2/B\ ,\\
\Delta C_{12}&=(K_1+k\sin^2\theta)(K_1+k\cos^2\theta)/B\ ,\\
\Delta C_{13}&=K_3(K_1+k\sin^2\theta)/B\ ,\\
\Delta C_{16}&=\tfrac{1}{2}k(K_1+k\sin^2\theta)\sin(2\theta)/B\ ,\\
\Delta C_{22}&=(K_1+k\cos^2\theta)^2/B\ ,\\
\Delta C_{23}&=K_3(K_1+k\cos\theta)/B\ ,\\
\Delta C_{26}&=\tfrac{1}{2}k(K_1+k\cos^2\theta)\sin2\theta/B\ ,\\
\Delta C_{33}&=K_3^2/B\ ,\\
\Delta C_{36}&=\tfrac{1}{2}kK_3\sin(2\theta)/B\ ,\\
\Delta C_{66}&=\tfrac{1}{4}k^2\sin^2(2\theta)/B\ .
\end{aligned} \tag{5.14}$$

These results show that the hexagonal symmetry of the lattice can be destroyed by coupling to the long-range antiferromagnetic order below T_N. In the zero-field case, an average over the magnetic domains of Fig. 1 gives the following results:

$$\begin{aligned}
\overline{\Delta C}_{11}&=\overline{\Delta C}_{22}=(K_1^2+K_1k+\tfrac{3}{8}k^2)/B\ ,\\
\overline{\Delta C}_{12}&=(K_1^2+K_1k+\tfrac{1}{8}k^2)/B\ ,\\
\overline{\Delta C}_{13}&=\overline{\Delta C}_{23}=\bar{K}K_3/B,\quad \overline{\Delta C}_{33}=K_3^2/B\ ,\\
\overline{\Delta C}_{66}&=\tfrac{1}{8}k^2/B
\end{aligned} \tag{5.15}$$

with all other $\overline{\Delta C}_{ij}=0$. As with $\Delta\alpha_i$, the small magnetic field required to obtain a single-domain state does not change the results (5.14) and predictions of the model for ΔC_{ij} with $\theta_a=0°$, $\theta_b=60°$, and $\theta_c=120°$ can be determined from these expressions.

Discontinuities in the thermal-expansion coefficients at $T=T_{N0}$ in the basal plane and along the c axis have recently been observed[25] (in zero magnetic field) in a needle-shaped sample[26] giving

$$\Delta\bar{\alpha}_{xx}\simeq-2.0\times10^{-6}K^{-1},\quad \overline{\Delta\alpha}_{zz}\simeq0.15\times10^{-6}K^{-1}\ .$$

Estimates of the magnetoelastic coupling coefficients can be obtained using these results and the relations (5.9) and (5.11) along with data for the elastic constants[27] (at 295 K) and the estimated value $a/B\simeq7.5\times10^4$ from Sec. IV A:

$$\bar{K}\simeq17.0,\quad K_3\simeq3.5 \tag{5.16}$$

in cgs units. An estimate for the parameter k (or K_1) is

not possible using zero-field thermal expansion data. Some of the elastic constant discontinuities predicted by the relations (5.15) can, however, be evaluated using the estimates (5.16) along with $B \simeq 5.9\times10^{-6}$ from Sec. IV A. The quantity $\overline{\Delta C}_{11}+\overline{\Delta C}_{12}$ depends on $\bar{K}$ and is given by $2\bar{K}^2/B$. It is thus possible to make the following predictions:

$$(\overline{\Delta C}_{11}+\overline{\Delta C}_{12})/(C_{11}+C_{12}) \simeq 1.5\times10^{-4} , \tag{5.17a}$$

$$\overline{\Delta C}_{13}/C_{13} \simeq 1.0\times10^{-4} , \tag{5.17b}$$

$$\overline{\Delta C}_{33}/C_{33} \simeq 2.2\times10^{-6} . \tag{5.17c}$$

These order-of-magnitude estimates appear to be consistent with the ultrasonic measurements of Ref. 25. Anomalous behavior in an elastic constant was found at T_{N0} giving an estimated discontinuity[26] $\Delta C/C \simeq 6\times10^{-5}$. Unfortunately, it was not possible to determine which sound mode was being measured although it is believed to contain elements of C_{44} and C_{11}. An interpretation that the data corresponds partially to a C_{11} mode is consistent with the results (5.17a). No anomaly in C_{44} at T_{N0} is predicted to occur as a result of the theory presented in this work. The only other elastic constant measured at T_{N0} was C_{33}. No anomaly is observed to one part in 10^5, which is consistent with the theoretical prediction (5.17c).

C. Applied stress

The effects of applying uniaxial stress on the long-range magnetically-ordered state of $CsNiF_3$ are considered here. Following the formalism given in Ref. 23, the Gibbs free energy

$$G = F - \sigma_i e_i \tag{5.18}$$

is considered, where σ_i is the stress tensor ($i=1-6$ and $\sigma_i>0$ corresponds to applied tension) and

$$F = A_Q S^2 + \tfrac{1}{2}BS^4 + \tfrac{1}{2}C_{ij}e_ie_j + \tilde{K}_i e_i S^2 . \tag{5.19}$$

At equilibrium, $\partial G/\partial e_i = 0$ and the result

$$e_i = s_{ij}(\sigma_j - \tilde{K}_j S^2) \tag{5.20}$$

follows from (5.18) and (5.19). The Gibbs free energy as a function of $\mathbf{S}$ and σ_i can be obtained using (5.20) in (5.18) with the result

$$G = G_0(T) + A_Q S^2 + \tfrac{1}{2}B'S^4 + \sigma_i s_{ij}\tilde{K}_j S^2 - \tfrac{1}{2}s_{ij}\sigma_i\sigma_j , \tag{5.21}$$

where

$$B' = B - s_{ij}\tilde{K}_i\tilde{K}_j . \tag{5.22}$$

This renormalization of the fourth-order coefficient $B \to B'$ is a consequence of magnetoelastic coupling only and occurs independent of the state of applied stress. In the analysis given in the previous sections of this work, it has been implicitly assumed that $B' \simeq B$. For $CsNiF_3$, with $\tilde{K}_i \lesssim 20$ and $s_{ij} \lesssim 10^{-11}$, this is seen to be a valid approximation since $B' \simeq 5.9\times10^{-6}$.

The effects of uniaxial stress on the orientation of the magnetic moments of Fig. 1 is similar to the magnetic-field effects discussed in Sec. IV A. Consider, for example, the application of stress along the y axis. Coupling between the orientation of $\mathbf{S}_1$ and stress is given by the fourth term of (5.21) with $\tilde{K}_i$ given by (5.6). Terms which depend on the angle θ between $\mathbf{S}_1$ and x axis are given by

$$F_{\sigma_2}(\theta) = k\sigma_2(s_{11}\cos^2\theta + s_{12}\sin^2\theta)S^2 \tag{5.23}$$

so that

$$\partial F/\partial\theta = -k\sigma_2(s_{11}-s_{12})\sin2\theta S^2 .$$

For $CsNiF_3$, $(s_{11}-s_{12})>0$ and $\theta=0$ minimizes the free energy if $k\sigma_2<0$. The sign of k is not yet known. These results indicate that if $k>0$ ($k<0$) then uniaxial compression (tension) applied along the y axis would tend to drive the crystal into a single-magnetic-domain state as shown in Fig. 1(a). For $k\sigma_2>0$, $\theta=90°$ minimizes (5.25), and the state shown in Fig. 4 should be stabilized at sufficiently large stress. For the case of applied hydrostatic pressure, $\sigma_i=-p$ for $i=1-3$, or stress along the c axis, the crystal remains in the three-domain state of Fig. 1.

The Néel temperature is also affected by the state of applied stress. The coefficient of the terms proportional to S^2 in (5.21) sum to zero at a temperature T_N given by

$$T_N = T_{N0} - a^{-1}\tilde{K}_i s_{ij}\sigma_j , \tag{5.24}$$

where $A_Q = a(T-T_{N0})$ has been used. For the case of applied stress along $\hat{\mathbf{y}}$ with $k\sigma_2<0$, so that $\theta=0$, the change in T_N with stress is characterized by

$$\partial T_N/\partial\sigma_2 = -a^{-1}[K_1(s_{11}+s_{12}) + ks_{11} + K_3 s_{13}] . \tag{5.25}$$

The relation (5.24) can also be used to show that for applied hydrostatic pressure

$$\partial T_N/\partial p = a^{-1}[2\bar{K}(s_{11}+s_{12}+s_{13}) + K_3(2s_{13}+s_{33})] , \tag{5.26}$$

and for stress applied along the c axis,

$$\partial T_N/\partial\sigma_3 = -a^{-1}[2\bar{K}s_{13} + K_3 s_{33}] . \tag{5.27}$$

Using the previously determined estimates for a, $\bar{K}$, and K_3 (along with data on the elastic constants[27]), the above theory can be used to make the following predictions:

$$\begin{aligned} &\partial T_N/\partial p \simeq 0.12 \text{ K/kbar} , \\ &\partial T_N/\partial\sigma_3 \simeq 4.4\times10^{-3} \text{ K/kbar} . \end{aligned} \tag{5.28}$$

Estimates for the stress dependence of the Néel temperature for other cases can be made only with a knowledge of the coefficient k.

D. Magnetostriction

Dilation of the crystal as a function of magnetic field is investigated here (also see Ref. 3). For the case where $\mathbf{H}$ is in the basal plane, contributions to the free energy which involve the induced uniform magnetization $\mathbf{m}$ can

be obtained from (5.1) using $\rho(\mathbf{r})$ given by (4.1). along with $\mathbf{s}(\mathbf{r})$ expressed by (3.2). The additional magnetoelastic terms are

$$F_{me}=\tfrac{1}{2}K_{10}(e_{xx}+e_{yy})m^2+\tfrac{1}{2}K_{30}e_{zz}m^2 +\tfrac{1}{2}k_0(e_{xx}m_y^2+e_{yy}m_x^2-2e_{xy}m_xm_y)\ , \tag{5.29}$$

where $K_{j0}=K_{jQ=0}$ and $k_0=k_{Q=0}$ [see (5.3) and (5.4)]. With the assumption that the magnetoelastic coupling coefficients are determined mainly by c-axis couplings, the approximations $K_{j0}\simeq K_{jQ}$ and $k_0\simeq k_Q$ analogous to the previous approximations for the coefficient B, can be made. Together with the $m=0$ terms given by (5.5), the total magnetoelastic energy can now be expressed as

$$F_{se}=\tilde{K}_ie_iS^2+\tfrac{1}{2}K_i'e_im^2\ , \tag{5.30}$$

where $\tilde{K}_i$ is given by (5.6) and

$$K_1'=K_1+k\beta_y^2,\quad K_2'=K_1+k\beta_x^2,\quad K_3'=K_3\ ,\quad K_4'=K_5'=0,\quad K_6'=-k\beta_x\beta_y \tag{5.31}$$

with β_x, β_y, β_z being the direction cosines of $\mathbf{m}$ (and $\mathbf{H}$) with respect to the crystallographic axes.

The change in the strain tensor induced by the magnetic field and long-range magnetic order is given by

$$e_i=-s_{ij}(\tilde{K}_jS^2+\tfrac{1}{2}K_j'm^2)\ . \tag{5.32}$$

The field dependence of e_i for cases where $\mathbf{H}$ is applied perpendicular to one of the magnetic domain orientations of Fig. 1 can be described using results for $S(H)$ and $m(H)$ of Sec. IV. It is assumed here that the field is of sufficient strength (e.g., $H>500$ Oe), so that the crystal is in a nearly single-domain state. Since $\mathbf{S}\perp\mathbf{m}$, the relations $\sin\theta=\beta_x$ and $\cos\theta=\beta y$ can be used to express the results as[3] for $H>H_c$

$$e_1=(J_1-\tfrac{1}{2}p)m^2\ , \tag{5.33a}$$

$$e_2=(J_1+\tfrac{1}{2}p)m^2\ , \tag{5.33b}$$

$$e_3=J_3m^2\ , \tag{5.33c}$$

$$e_6=\tfrac{1}{2}ks_{66}\beta_x\beta_ym^2\ ; \tag{5.33d}$$

for $H<H_c$,

$$e_1=(J_1-\tfrac{1}{2}p)\chi^2H_c^2+p\chi^2(H_c^2-H^2)\ , \tag{5.34a}$$

$$e_2=(J_1+\tfrac{1}{2}p)\chi^2H_c^2-p\chi^2(H_c^2-H^2)\ , \tag{5.34b}$$

$$e_3=J_3\chi^2H_c^2\ , \tag{5.34c}$$

$$e_6=\tfrac{1}{2}ks_{66}\beta_x\beta_y\chi^2[H_c^2-2(H_c^2-H^2)]\ ; \tag{5.34d}$$

where

$$J_1=-\tfrac{1}{2}[\bar{K}(s_{11}+s_{12})+K_3s_{13}]\ ,\quad J_3=-\tfrac{1}{2}[2\bar{K}s_{13}+K_3s_{33}]\ ,\quad p=k(s_{11}-s_{12})(\beta_y^2-\tfrac{1}{2})\ , \tag{5.35}$$

and $e_4=e_5=0$. For $H>H_c$, $m(H)$ in (5.33) is determined by the solution of (4.5). Note that for $H<H_c$, e_3 is predicted to be independent of the field and that the quadratic field dependence of e_1 and e_2 is proportional to the parameter $p\propto k$, which is therefore expected to be weak. Numerical estimates for J_1 and J_3 can be obtained using $\bar{K}$ and K_3 given by (5.16) with the result (in cgs units)

$$J_1\simeq-1.3\times10^{-11},\quad J_3\simeq-9.7\times10^{-13}\ . \tag{5.36}$$

Finally, we consider magnetostriction for the case with $\mathbf{H}$ is along the c axis, where the three-domain spin structure of Fig. 1 remains unperturbed. Additional terms must be added to F_{me} given by (5.29) which are invariant under hexagonal symmetry (for this case where $\mathbf{m}\|\hat{\mathbf{z}}$) given by

$$F_{me}^z=\tfrac{1}{2}k_1(e_{xx}+e_{yy})m_z^2+\tfrac{1}{2}k_3e_{zz}m_z^2\ . \tag{5.37}$$

The independent coefficients k_1 and k_3 have not been previously introduced. Using the results and approximations given in Sec. IV B, with H_{cz} given by (4.20), the field dependence of the strain tensor can be shown to have the following behavior for $H>H_{cz}$,

$$e_1=e_2\simeq(J_1+u)\chi_z^2H^2\ ,\quad e_3\simeq(J_3+v)\chi_z^2H^2\ , \tag{5.38}$$

for $H<H_{cz}$,

$$e_1=e_2\simeq(J_1+u)\chi_z^2H_{cz}^2+(J_1b_1-u)\chi_z^2(H_{cz}^2-H^2)\ ,\quad e_3\simeq(J_3+v)\chi_z^2H_{cz}^2+(J_3b_1-v)\chi_z^2(H_{cz}^2-H^2)\ , \tag{5.39}$$

and $e_4=e_5=e_6=0$, where b_1 is defined in (4.18), χ_z by (4.19), and

$$u=-\tfrac{1}{2}[(k_1-\tfrac{1}{2}k_3)(s_{11}+s_{12})+k_3s_{13}]\ ,\quad v=-\tfrac{1}{2}[2(k_1-\tfrac{1}{2}k_3)s_{13}+k_3s_{33}]\ . \tag{5.40}$$

These results differ from the corresponding basal-plane expressions (5.33)–(5.35) by the introduction of new parameters u and v and by the prediction of quadratic field dependence in the region $H>H_{cz}$.

E. Inhomogeneous strain

We have also investigated the possibility that the long-range antiferromagnetic ordering in $CsNiF_3$ can induce a periodic distortion of the lattice. The appropriate magnetoelastic coupling which involves $\delta e_{\alpha\beta}(\mathbf{r})$ of (2.5) is simply a generalization of the form (5.1), and can be derived from (2.3). In analogy with $\mathbf{s}(\mathbf{r})$ written in the form (3.2) and (3.3), we define (also see Ref. 3)

$$\delta e_{\alpha\beta}(\mathbf{r})=\frac{1}{2}\frac{V}{N}\sum_{\mathbf{R}}\left[\frac{\partial u_\alpha}{\partial r_\beta}+\frac{\partial u_\beta}{\partial r_\alpha}\right]\delta(\mathbf{r}-\mathbf{R}) \tag{5.41}$$

with the lattice displacement [from the zero-field paramagnetic configuration $\mathbf{u}(\mathbf{r})$] expressed by the Fourier sum

$$\mathbf{u}(\mathbf{r})=\sum_{\mathbf{q}}\mathbf{U}_\mathbf{q}e^{i\mathbf{q}\cdot\mathbf{r}}\ . \tag{5.42}$$

With these definitions, the elastic energy F_e and the mag-

netoelastic energy F_{se} can be expressed in terms of the polarization vectors $\mathbf{U}_q$ and $\mathbf{S}$. For the zero-field case, it can be shown that F_{se} is zero as a consequence of the magnetic ordering being antiferromagnetic. In the presence of an applied magnetic field, the free energy is minimized with $\mathbf{U}_q=0$. No inhomogeneous strain is thus predicted to occur in $CsNiF_3$.

VI. CONCLUSIONS

A versatile nonlocal free-energy functional, based on the Landau theory of phase transitions, has been developed in this work and used to describe a variety of properties associated with the low-temperature magnetic ordering of $CsNiF_3$. The nonlocal character of this model differs from usual expressions of the Landau free energy and is crucial for a complete treatment of phase transitions to ordered phases, which can exhibit a wide variety of structure. The utility of this approach is that it provides a general starting point from which the development of a Landau free energy can be made appropriate for the study of specific systems, characterized by symmetry. The application of this formalism to correctly predict the three-domain antiferromagnetic structure of $CsNiF_3$ has been demonstrated in Sec. III of this work. This structure was shown to be a consequence of strong magnetic dipole-type coupling (corroborating the work of Refs. 14 and 15) which enters the free energy in a nonlocal form.

The strong anisotropy between the c axis and basal plane plays an important role in determining the behavior of the magnetic and elastic properties of this hexagonal crystal. These effects account for the alignment of the magnetic moments in the basal plane and the ferromagnetic character of the ordering along the c axis, as well as the anisotropic behavior predicted and observed for the critical field $\mathbf{H}_c$, field-induced magnetization $m(\mathbf{H})$, and all of the magnetoelastic properties.

A major focus of this work has been an investigation of the effects of magnetic domain reorientation under the influence of a magnetic field applied in the basal plane. A crystal with predominantly only one of the three domains can be achieved by applying a small field. The calculated elastic properties are then predicted to depend on the orientation of the magnetic moments through the magnetoelastic coupling parameter k. Experiments have not yet been performed, which would show these effects and enable a numerical estimate of k to be made by a comparison with the corresponding theory. A good candidate for such a comparison is magnetostriction, using sensitive dilatometry where quadratic field dependence proportional to k is predicted for $H<H_c$. Although magnetic-moment orientation is also predicted to influence results for the discontinuities in the thermal-expansion coefficients and the elastic constants at T_N, these effects may be obscure if k is small, as may be the case. The theory presented in this work is not applicable for the study of the field dependence of properties in the very small field regime ($H<500$ Oe) where the crystal consists of the three magnetic domains of unequal size. A theory of thermodynamic properties for these field strengths requires a detailed analysis of the dependence of the domain wall sizes on the field.

The theory was also used to study the influence of uniaxial stress on magnetic-moment orientation, and it was shown that a single-domain state can be achieved in analogy with the application of a magnetic field. Expressions for the stress dependence of the Néel temperature were also derived with the result that these moment-orientation effects also depend on the parameter k. These results also suggest that sample-dependent internal stresses may influence the relative size of the three magnetic domains and therefore could affect the experimental results for many thermodynamic properties.

Even though no explicit calculation is pursued here, it is interesting to envisage the possibility of measuring the magnetic properties of $CsNiF_3$ through dielectric and optical methods. The magnetic contributions to the birefringence[28,29] should be affected by the application of a magnetic field or stress. Direct refractive index measurements are also a candidate to probe magnetostriction and applied stress effects through the modifications of the photo-elastic coefficients.

As indicated in the Introduction, the rich variety of phase transitions which can occur in ABX_3-type compounds offers many possibilities for the application of the nonlocal Landau theory presented in this work. An investigation of the magnetic phase diagram of $CsNiCl_3$ has recently been completed.[30] Work is in progress on a description of the magnetic phase transitions in $CsCoCl_3$ and $CsCoBr_3$ based on the Landau free energy. A study of what appears to be a structural phase transition[25] at 190 K in $CsNiF_3$ is also planned.

ACKNOWLEDGMENTS

This research is supported by the Natural Sciences and Engineering Research Council of Canada and Le Fonds Formation de Chercheurs et l'Aide à la Recherche (FCAR) du Québec.

APPENDIX

Including up to third-neighbor interactions for D_Q, $D_{z,Q}$, and $d_Q^{\alpha\beta}$ given by (3.5), (3.10), and (3.11) leads to the following form for the free energy at order S^2 [see (3.15)]:

$$
\begin{aligned}
F_s^{(2)}=&\{2J_c+D_c+(2J_a+2D_1+d_1)[\cos x+2\cos(\tfrac{1}{2}x)\cos y]+(2D_2+3d_2)[\cos(2y)+2\cos(y)\cos(\tfrac{3}{2}x)]\\
&+(2D_3+4d_3)[\cos(2x)+2\cos x\cos(2y)]\}S^2\\
&+(\cos 2\theta\{d_1[\cos x-\cos(\tfrac{1}{2}x)\cos y]+3d_2[\cos(y)\cos(\tfrac{3}{2}x)-\cos(2y)]+4d_3[\cos 2x-\cos x\cos(2y)]\}\\
&+3^{1/2}\sin 2\theta\{d_1\sin(\tfrac{1}{2}x)\sin y+3d_2\sin y\sin(\tfrac{3}{2}x)+4d_3\sin x\sin(2y)\})S^2\Delta_{2\mathbf{Q},\mathbf{G}_1}\,, \qquad \text{(A1)}
\end{aligned}
$$

where

$$x = aQ_x, \quad y = bQ_y ,$$

$$D_n = \tilde{D}(\mathbf{R}_n) + \tilde{D}_z(\mathbf{R}_n) ,$$

and $d_n = \tilde{d}(\mathbf{R}_n)$ with $\mathbf{R}_n$ equal to the nth-neighbor distance in the basal plane. For $\mathbf{Q} \neq \frac{1}{2}\mathbf{G}_1$, minimization of (A1) gives $(x,y) = (4\pi/3, 0)$ or $(2\pi/3, \pi)$ if $j > 0$, where

$$j = J_a + D_1 + \tfrac{1}{2}d_1 - 6D_2 - 9d_2 + 4D_3 + 8d_3 \qquad \text{(A2)}$$

and $(x,y) = (0,0)$ for $j < 0$. For $\mathbf{Q} = \frac{1}{2}\mathbf{G}_1$, angles θ (between the spin vector and the x axis) equal 0°, 60°, 120° for $\mathbf{Q}_a$, $\mathbf{Q}_b$, and $\mathbf{Q}_c$ [given by (3.18)], respectively, minimize the free energy provided that $(d_3 - 3d_2) < 0$. A comparison of the free energies for the 120° structure and antiferromagnetic orderings shows that for

$$j < (2D_2 - 5D_3 - 2d_1 + 9d_2 - 10d_3) \qquad \text{(A3)}$$

the antiferromagnetic structure (Fig. 1) of $CsNiF_3$ is stabilized, and for j greater than this quantity the 120° ordering is realized.

[1] J. C. Toledano and P. Toledano, *The Landau Theory of Phase Transitions* (World-Scientific, Singapore, 1987).

[2] See, e.g., R. A. Cowley, Adv. Phys. **29**, 1 (1980); Yu. A. Izyumov, Usp.Fiz. Nauk. [Sov. Phys. Usp. **27**, 845 (1985)].

[3] That nonlocal terms in the free energy can be important has been noted by, e.g., M. B. Walker, Phys. Rev. Lett. **44**, 1261 (1980); M. L. Plumer and M. B. Walker, J. Phys. C **15**, 7181 (1982); also see Ref. 19.

[4] J. A. Kafalos and J. M. Longo, Mater. Res. Bull. **3**, 501 (1968).

[5] A. Gomez Cuevas, J. C. Launay, J. M. Perez Mato, J. Fernandez, A. Lopez, and M. J. Tello, Ferroelectrics **55**, 121 (1984).

[6] P. C. Donohue, L. Katz, and R. Ward, Inorg. Chem. **4**, 306 (1965).

[7] X. Zhu and M. B. Walker, Phys. Rev. B **36**, 3830 (1987).

[8] N. Wada, K. Ubukoshi, and K. Hirakawa, J. Phys. Soc. Jpn. **51**, 2833 (1982).

[9] M. Steiner, J. Villain, and C. G. Windsor, Adv. Phys. **25**, 87 (1976).

[10] M. Steiner and H. Dachs, Solid State Commun. **9**, 227 (1971).

[11] M. Steiner and J. K. Kjems, J. Phys. C **10**, 2665 (1977); C. Dupas and J.-P. Renard, *ibid.* **10**, 5057 (1977).

[12] M. Steiner, Solid State Commun. **11**, 73 (1972).

[13] M. Steiner and H. Dachs, Solid State Commun. **14**, 841 (1974).

[14] C. Scherer and Y. Barjhoux, Phys. Status Solidi B **80**, 313 (1977).

[15] N. Suzuki, J. Phys. Soc. Jpn. **52**, 3199 (1983); H. Shiba and N. Suzuki, *ibid.* **51**, 3488 (1982).

[16] M. E. Fisher, S.-k. Ma, and B. G. Nickel, Phys. Rev. Lett. **29**, 917 (1972); also see G. Toulouse and P. Pfeuty, *Introduction au Groupe de Renormalisation et a ses Applications* (Presses Universitaires, Grenoble, 1975).

[17] J. V. Lebesque, J. Snel, and J. J. Smit, Solid State Commun. **13**, 371 (1973).

[18] X. Zhu and M. B. Walker, Phys. Rev. B **34**, 8064 (1986).

[19] D. Babel, Z. Anorg. Allg. Chem. **369**, 117 (1969).

[20] Also see M. L. Plumer and M. B. Walker, J. Phys. C **14**, 4689 (1981).

[21] Ch. Rosinski and B. Elschner, J. Mag. Mag. Mat. **4**, 193 (1977).

[22] H. Yamazaki, E. Soares, H. Panepucci, and Y. Morishige, J. Phys. Soc. Jpn. **48**, 1453 (1980).

[23] M. B. Walker, Phys. Rev. B **22**, 1338 (1980).

[24] H. Yamazaki, E. Soares, H. Panepucci, and Y. Morishige, J. Phys. Soc. Jpn. **47**, 1464 (1979).

[25] A. M. Simpson, A. Caillé, and M. Jericho, Solid State Commun. **64**, 1117 (1987).

[26] It is likely measured values of elastic properties are sample dependent due to the influence of internal stresses on the magnetic domain structure (see Sec. VI).

[27] F. Ganot, C. Dugautier, P. Moch, and J. Nouet, Solid State Commun. **44**, 975 (1982).

[28] J. Ferré and G. A. Gerhing, Rep. Prog. Phys. **47**, 513 (1984).

[29] T. Levola and W. Kleemann, J. Phys. C **18**, 1513 (1985).

[30] M. L. Plumer, K. Hood, and A. Caillé, Phys. Rev. Lett. **60**, 45 (1988).